



A Low-Cost Upper Limb Exoskeleton for Rehabilitation
and Constrained Movements for Sports

Jinhang Li

A thesis submitted in partial fulfilment of the requirements
for the degree of MRes in Medical Robotics and Image
Guided Intervention and for the Diploma of Imperial
College

Imperial College London

December, 2020

Supervisor: Benny Lo

Co-Supervisor: Rejin John Varghese

Acknowledgements

I would like to acknowledge my supervisor Dr. Benny Lo to host my master degree and funding supply to my individual research. Also, I would like to thank my co-supervisor Rejin John Varghese for his technical support.

I want to especially thank my parents and family members. Without their support and care, there would be no achievements I have achieved today.

Finally, I would also like to thank my classmate JinShi Zhao for his help and friendship.

List of Abbreviations:

ROM-Range of Motion

ADL- Activity of Daily Living

EMG- Electromyography

FRS- Force Resistance Sensor

CAD- Computer Aided Design

FEA- Finite Element Analysis

IMU-Initial Measurement Unit

MEMS- Microelectromechanical systems

RNN-Recurrent neural network

LSTM- Long short-term memory

GRU- Gated recurrent units

Bid-Bidirectional

ANN- Artificial Neuro Network

CNN-Convolutional Neuro Network

Act. - Activation Function

MSE- Mean Square Error

RMSE- Root Mean Square Error

IQR- Interquartile Range

Abstract

Most of the daily activities of human beings require upper limbs to complete. **Neurological diseases** (such as stroke) and sports injuries will cause upper limb movement limitation. For post stroke rehabilitation, the current use of exoskeleton equipment can reduce costs and achieve recovery effects. However, for the prevention of upper limb sports injuries, only passive brace and band are the only way to prevent injuries. Combining these two points, this work is to design an exoskeleton that can meet both needs at the same time. For this reason, a **rigid exoskeleton with a single degree of freedom** is proposed based on 3d printing, and the **two control principles correspond to two applications.**

Background(Literature Review):

Human beings have flexible upper limbs, which enables people to create new things. The human upper limbs play an important role in daily life. People cannot do most of daily tasks without the assistance of their upper limbs. However, the function of human upper limbs is easily affected. This is divided into internal factors and external factors. Internal factors include, for example, neurological diseases caused by stroke, which leads to attenuation of upper limb motor function. The external factors include injury during exercise, which leads to the limitation of upper limb movement. Therefore, the purpose of this project is divided into two, one is to improve upper limb movement caused by neurological diseases represented by stroke, and the other is how to avoid the influence of upper limb movement caused by sports injuries.

For the disease of stroke, it not only causes limitation of movement, but also one of the main diseases that cause death, there are approximately 700,000 stroke cases occur each year in the United States, of which nearly 165,000 people die from strokes [1]. The number of stroke cases per year is still increasing, it may increase by 30% until 2025s [2]. Survivors after a stroke are accompanied by some sequelae such as hemiplegia which presents persisting disabilities or restricted movement of the upper and lower limb [3]. Fortunately, because of the nature of neuroplasticity. The nervous system's control of limb movement can be improved with daily physical rehabilitation tasks.



Fig. 1 Mirror Therapy of Hand Rehabilitation for post-stroke patient <https://www.flintrehab.com/mirror-therapy-stroke/>

However, rehabilitation techniques only have a good positive effect at a certain period of time after stroke. Especially for upper limb recovery which has shorter “golden period” to recovery, the “golden period” for upper limb recovery is about 11 weeks after stroke [4]. H. Nakayama et al. [5] found that further recovery will be not expected if pass the

“golden period”. Therefore, opportune rehabilitation exercises are necessary for patients’ recovery.

The basic concept of the rehabilitation techniques is aimed to make motor recovery based on the neural plasticity. This process is carried on by repeating training for some specific tasks in order to recover the function of corresponding limbs, the rehabilitation process for post-stroke patients need to be designed and assisted with a team of therapists [6,7,8]. The training task and training facilities (i.e. rehabilitation robotics) will be different for the different patients because their different learning functions may be injured [9]. At present, the most commonly used rehabilitation training method is mirror therapy. Fig.1 shown the example of mirror therapy, its mechanism is to use the reflection of the mirror to create the phantom of the affected limb to deceive the brain, it could reduce the pain of the affected limb and improve motor function. However, the labour cost of the therapist is usually expensive, especially during long treatment periods [11,12]. Therefore, a portable, cheap and efficient treatment for post-stroke has become necessary in order to decrease the cost of post stroke rehabilitation.

The sport injuries often caused by sudden violent impacts or exceeding the ROM of the limbs. It can cause muscle strained or strained ligaments and fractures. Moreover, exercise or manual labour can cause many chronic diseases. For example, tennis players often get injuries of elbow joint due to the impact of the tennis ball [62].

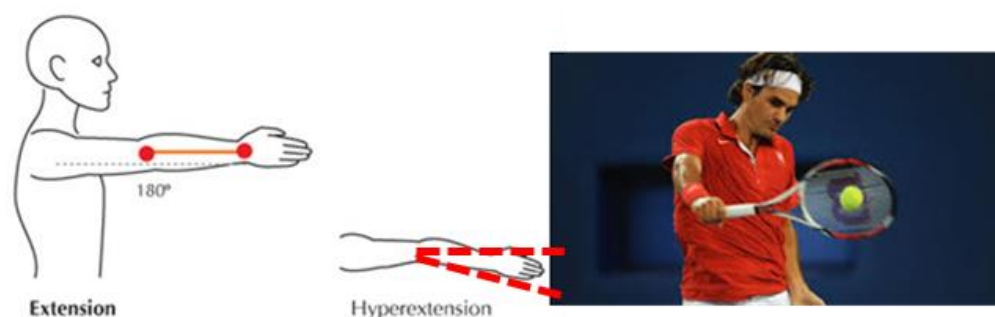


Fig. 2 Schematic of the elbow over extension while playing the tennis

For the tennis players there are some common injuries such as elbow overextension, lateral epicondylitis also known as tennis elbow. But for novices and elder tennis players are more likely to have elbow overextension. The normal range of motion of elbow joint is up to 180 degree at fully extension posture. Fig.2 shown the schematic of the elbow over extension while playing the tennis. The definition of elbow overextension is the elbow angle is larger than 180 degree at fully extension posture when swing the tennis racket. For elder player, the strength muscle group around

elbow are weaker than the young player. And the novice's players don't have a good motion control when play the tennis. Therefore, it is more likely to get injuries for these two groups. As the tennis always has heavy and rapid motion if the players always do it at overextension posture. It would easily cause the injury of the ligament. There are some passive elbow band to prevent the elbow overextension shown in Fig.3 . However, it need to be tight Therefore, an effective way to prevent elbow joint overextension could be wearing a wearable mechanical device that can operate automatically.



Fig. 3 Elbow Brace <https://www.amazon.com/Immobilizer-Pediatric-Tendonitis-Stabilizer-Restraints/dp/B08HGHPQZ5>

1. Upper Limb Ergonomics:

Wearable mechanical devices have to move follow the biological movement of the limb. Otherwise, the mechanical part may hurt the limb. Therefore, demonstration of limb ergonomics and range of motion (ROM) for activity of daily living (ADL) are necessary to mechanical design for wearable robotics.

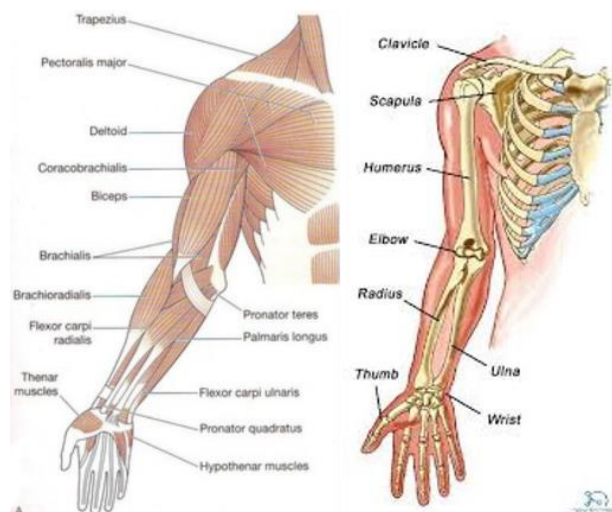


Fig. 4 RHS Upper Limb, (left) Muscle Map, (right) skeleton and joints [13]

The human upper limbs consisted with wrist, elbow joint and shoulder complex. The skeletons and muscle map for upper limb shown in Fig 4. The ROM of upper limb are constrained by the ligament which could prevent the dislocation and skeletons stability [14]. In this section, the hand part is neglected (but the wrist included in this section).

The shoulder complex consisted with four independent joints: sternoclavicular joint, acromioclavicular joint, glenohumeral joint and scapulothoracic joint [15]. The coordinated motion those shoulder joints allows the upper limb movements for ADLs about shoulder complex such as flexion, abduction and adduction [16]. The shoulder joint has three DOFs but the number of DOFs could increase as the axis of rotation deviated [17]. S. Namdari et al. [18] investigated the ROM of the shoulder joint when 18 male subjects and 2 female subjects doing ten different ADLs separately. The result provided that the ROM of the shoulder shown in Table 1. Wrist joint is also a complex one compare with elbow joint. Most of human ability to use tools comes from fine control of the wrist and hand. The wrist joint constructed with radial wrist joint, intercarpal joint and carpometacarpal joint [19]. The wrist joint has two DOFs which allows hand moving about the wrist. J. Ryu et al. [20] conducted an experiment about ROM of wrist joint. The experiment was carried out with 40 subjects (20 males and 20 females). The experimental results yielded the active ROMs of wrist: [Extension: 60°; Flexion: 54°; Ulnar Deviation: 40°; Radial Deviation: 17°]. Elbow joint consists of the distal humerus and the proximal ulnar articular surface. Structurally, it consists of three joints in structure which are enclosed in a joint capsule [21]. The elbow joint existence allows flexion, extension, and forearm rotation. The elbow joint has active ROMs: [Flexion: 60°; Extension: 180°; Supination: 85°; Pronation: 75°] [22].

Motion of Shoulder	ROM
Flexion	$121^{\circ} \pm 6.7^{\circ}$
Extension	$46^{\circ} \pm 5.3^{\circ}$
Abduction	$128^{\circ} \pm 7.9^{\circ}$
Cross-body adduction	$116^{\circ} \pm 9.1^{\circ}$
External rotation with arm 90° abducting	$59^{\circ} \pm 10^{\circ}$
Internal rotation with the arm at the side	$102^{\circ} \pm 7.7^{\circ}$

Table 1 ROM of Shoulder from [56]

2. Actuation Techniques:

Recently, the exoskeleton for rehabilitation and other applications has been developed very widely and still developing. Moreover, the exoskeleton has already become

commercial. The representative one such as HAL-3 post-stroke therapy has been widely used [23,24]. Clinical studies provided the evidence that wearable assistive robot could improve motor function of hand significantly [25]. The benefits of exoskeleton can precisely control of limbs movement and portable size [26]. Therefore, it could satisfy daily frequent training command of patient as a wearable robotics for rehabilitation [27]. However, according to the literatures, there is no such active exoskeleton to prevent the This section is to demonstrate the actuation techniques from other literatures about exoskeleton.

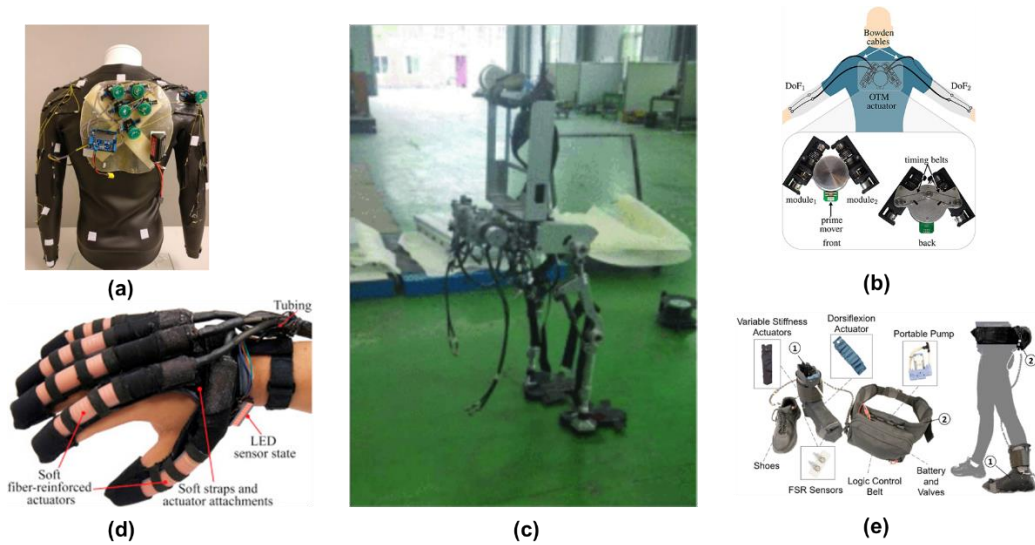


Fig. 5 (a) CRUX [28], (b) OTM transmission structure [29], (c) CASWELL-II [30], (d) Soft exoskeleton for hand assistance and rehabilitation [31], (e) Soft exoskeleton for foot drop assistance [32].

3.1. Motor-Cable Drive Line:

This mechanical structure mainly constructed with motor and driven cable (tendon) and the power resource always be battery. The rotation of motor transfer into a linear movement which provide a certain amount of torque to the limbs so that it could assist the limb motion. The advantage of the motor actuation is more accurate and better controllability than other types of actuators (i.e. hydraulic actuator, pneumatic actuator, etc.) [33]. For an instance, CRUX [28] designed for post-stroke patient's rehabilitation which shown in Fig 5(a). The CRUX soft exoskeleton has 6 brushed DC micromotors, 5 placed on the back plate and the 6th motor placed nearby the shoulder where the limb is weaker than the other side. It powered by a three-cell 3500mAh lithium polymer battery which could provide 12.6 volts and 50 Ampere at most. The material of driven cable was made by braided aramid which is capable to carry 220N load. This system used the Bowden Shell guide the cable to where the limb should be attached. The CRUX system could drive both arms and provide more power for the weaker side to achieve the Mirror Therapy. However, this design may cause limited movement

because the position and number of motors are customized based on the set limb movements [35]. M. Xiloyannis et al. [37] introduced a motor-cable driven soft exoskeleton based on One-To-Many (OTM) transmission structure, the exoskeleton shown in Fig 5(b). It assists same limbs as CRUX. The difference to this exoskeleton is that only actuated by a Maxon EC-i 40 DC motor which could produced max power 70 w at 3.6:1 reduction ratio. The OTM structure consisted with three EM clutches so that power of motor could transit to both arms, EM clutch also allows the robotics to operate in three states: forward-driving, back-driving and lock state. It could ensure the magnitude and direction of output torque to limbs by controlling the energized state of EM clutch. However, it is heavier than the CRUX due to more metal transmission structure included. Therefore, lightweight design should be developed.

3.2 Hydraulic and Pneumatic Drive Line:

The main benefit of hydraulic actuators is the small size to power ratio. It means that it could produce more power than other actuators (i.e. motor) at the same size of structure [28]. Also, it has good compliance and relative lower inherent stiffness [22]. In traditional rigid exoskeleton, hydraulic actuators usually use a single hydraulic cylinder to drive two segments to perform 1DOF activities. For an instance, Y. Yang et al. [25] introduced a hydraulic actuated exoskeleton for leg assistance called CASWELL-II which shown in Fig 5(c). It utilized a hybrid electro-hydraulic actuators system as the power actuation method. The hybrid electro-hydraulic system constructed with a magnetic fluid valve and a unidirectional servo fluid valve. The actuation achieved by adjusting the displacement from original state of piston in the cylinder by the hybrid electro-hydraulic system. However, rigid hydraulic cylinders are not suitable to be used directly for soft exoskeleton due to the softness and mechanical design of soft exoskeleton. P. Polygerinos et al. [26] invented a soft exoskeleton for hand assistance and rehabilitation which shown in Fig 5(d). Instead of rigid hydraulic cylinder, they constructed a multi-segment soft actuator which made of silicone material to allow multiple DOFs movement of hand. The entire hydraulic system carried with a waist pack which is portable. It constructed with a (5Ah, 14.8 V) lithium polymer battery to be a power resource and 250ml water reservoir. The maximum pressure and output power of the water pump were 340kpa and 9.8w respectively, and the solenoid valves switch on/off the actuator. The total weight on the waist package was 3.3kg. The valve controls the water into the actuator's internal cavity to deform it, thereby generating a driving force to assist the flexion and extension of the hand joint. The system successfully achieve assistance of grasping a bottle of water, telephone and independent movement of thumb, index and small thumb finger. However, there was

a delay about 30ms of response time due to the resistance between water and actuator. Pneumatic actuation technology is similar with hydraulic actuation.

Pneumatic actuation uses air as the fluid to be the actuation media and it needs an air compressor. C. Thalman et al. [39] introduced a soft exoskeleton for foot drop assistance application which shown in Figure 5(e). The whole power and control system packed on the waist belt which was 1.6kg. The power resource was a set of 11.1V LiPo batteries which supplied the power to the air pump. This system was testing at 25°C environment. The dorsiflexion actuator was inflatable fabric-based could tow the toe to lift the feet and the actuator uniaxial contraction lead the feet lifting. However, the air pressure was sensitive to the temperature change. Therefore, this system can only be used in a constant temperature environment such as indoors, thereby the liquid hydraulic are more suitable at outdoor environment.

3. Features of Sensing Techniques:

For the exoskeleton device, the core is how to obtain the user's intention, which is converted into the corresponding electrical signal to the actuator through the control algorithm. This can be divided into three categories, one of which is to obtain movement intention directly through biological signals, such as the use of EMG sensors or EEG sensors to directly obtain electrical signals from muscles or brains.

The characteristic of this sensing technique is that it is based on the electrical signals of human tissues to obtain the movement status of the limbs, such as EMG sensors. When muscles contract, weak electrical signals are generated and captured by the sensors. However, the disadvantage is that the EMG signal is often accompanied by noise, because when the limbs make movements, it is the result of the muscle group, so the EMG signal generated by the nearby muscle group will also be captured [37].

The other one is to obtain the current motion scene through an external sensor (i.e. FRS, Flex sensor etc.), thereby indirectly obtaining the motion intention through an algorithm. The characteristic of this sensing technique is that it is based on the electrical signals of human tissues to obtain the movement status of the limbs, such as EMG sensors. When muscles contract, weak electrical signals are generated and captured by the sensors. However, the disadvantage is that the EMG signal is often accompanied by noise, because when the limbs make movements, it is the result of the muscle group, so the EMG signal generated by the nearby muscle group will also be captured [32,31]. The third category is based on the sensor fusion. The characteristic of this method is that it can infer the user's movement intention based

on multiple sensors. Because it combines the advantages of multiple sensors, the control output is more accurate [35].

Conclusion:

According to the literatures, the common actuator for post stroke rehabilitation application is electric motor which could provide accurate output. And the soft wearable robotics such as CRUX became more popular recently. However, the soft wearable robotics is always expensive, due to the tendon cost, does not satisfy the requirement of low cost. And the sensor fusion technology could provide the most accurate motion trajectory. However, more sensors need more cost which also goes against to the low cost requirement. Most importantly, there is no active wearable robotics device for elbow overextension prevention. Therefore, this project aimed to design a low cost rigid exoskeleton with motor actuator and indirect sensitivity technique for both post-stroke rehabilitation application and tennis service constrain

Exoskeleton Design:

The rigid design software is designed based on the CAD software. The design limitation is based on the size of human subjects' upper limb. Because the exoskeleton needs to match with the dimension of the limb to avoid interfacing to the limb motion. Fig. 6 shown the anatomy image of the upper limb muscle at the extension and flexion posture. Scenario (a) shown the muscle deformation when the elbow is fully extending with the direction of the red curve arrow. The triceps muscle bicep contracted to produce the torque allows the elbow to extend with the triceps muscle volume expanding. The elbow joint flexion scenario shown in (b) and the blue narrow shown the direction of biceps contraction to produce the elbow flexion at the direction of red curve. The black line of the fixed point represents the area of tendons of biceps and triceps of upper arm nearby the shoulder joint. At this area, the volume difference of the muscle at flexion and extension situation are negligible compared with the centre of the biceps and triceps muscle.

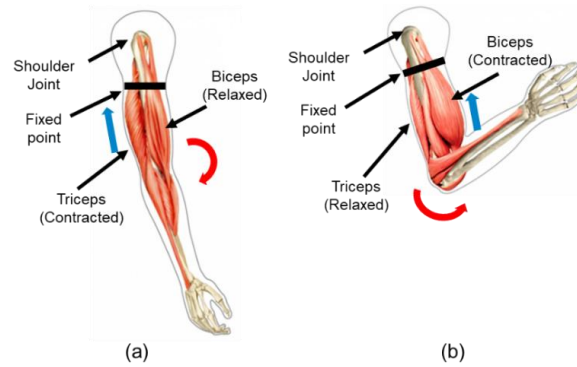


Fig. 6 Anatomy of Upper Limb [40],

(a) scenario of the elbow extension, (b) scenario of the elbow flexion

Therefore, the part of exoskeleton fixed on the upper limb is expected around the fixed point of the upper limb for the human subjects, and the width of fixing part also needs to equal or smaller than the space between fixed point area and the shoulder joint. The Fig. 7 shown the picture of the upper limb and the dimension of the upper limb for a human subject (a 22 -years-old male teenager with height of 175cm). The dimension for the limb dimension was measured by the tape measure. The distance between the fixed-point area and the elbow joint is about 105.92mm along the limb. The distance between the elbow joint to the wrist joint is about 234.89mm.

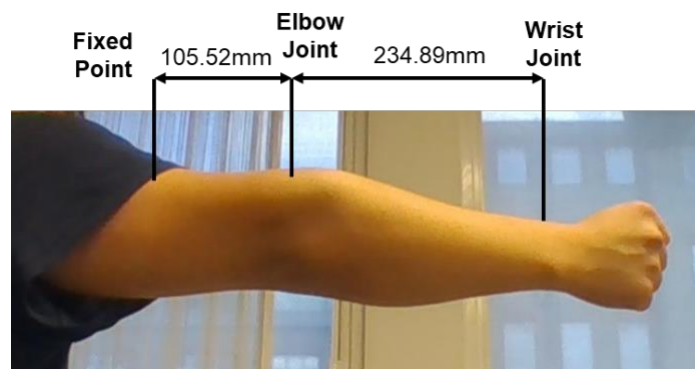


Fig. 7 Human Subject Right Upper Limb Dimensions

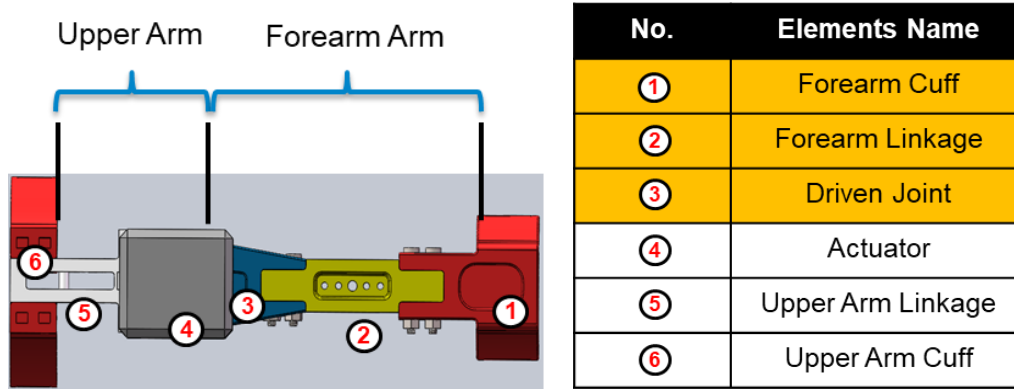


Fig. 8 CAD Design for the upper limb

Table 2 Parts list for exoskeleton

The CAD design for upper limb is accomplished by the Solidworks 2019. Fig. 8 shown the CAD model and element numbers for the limb which is divided into two parts upper arm part and forearm part. There are totally five separately elements for the CAD design of the rigid exoskeleton. The part 4 represents the schematic of the actuator which is located at the area of the elbow joint. Table 2 shown the number of parts and the corresponding element names, and the highlighted parts means the main elements where the loading applied.

The 3D printing is chosen as the manufacturing method for the exoskeleton elements. The main advantage of utilizing 3D printing manufacturing is it has ability to manufacture different shape in several hours so that it could allow edit the parts efficiently. Compare with traditional CNN manufacturing method it could minimize the waste of material. Most importantly, it allows to print the parts made by plastic material with enough strength and light weight [41]. A Tier Time Up Mini has been used as the 3D printer equipment for this project. It has the printing platform with maximum area of printing 120mm × 120mm, and the nozzle diameter is 0.4mm with 0.15mm of the printing tolerance.

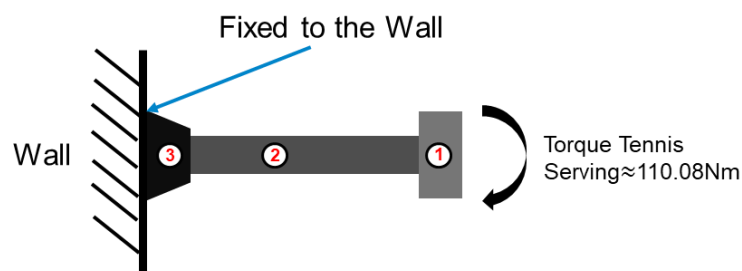


Fig. 9 Schematic Representation of Torque Applied to the Forearm Part

The ABS plastic material has been specified into the printing material. This type of material has the benefits of light weight and high tensile strength of parts used for mechanical application, it also very resistance to corrosion and oxidation. Therefore, it is suitable for wearable exoskeleton application because the human always sweating while doing exercise. Body fluid may age the material which directly contact to it, then fracture the parts for long-term usage [42]. However, the FEA test should be applied to the CAD model so that to ensure the structure with specific ABS material could stand the load before manufacturing. Fig. 9 shown the schematic representation of the elbow torque applied on the Forearm Part of the exoskeleton with the Driven joint is fixed to the wall. The simulation stress applied on the forearm part should be equal to the stress caused by the elbow joint torque motion while one end of the part is fixed, in order to ensure the elements will not break while the part suddenly stand the possible extreme largest load. According to the literature, the torque for the tennis serving could reach to around 110.08 Nm. Table 3 shown the FEA results for the three elements for the forearm part. It could be seen that the maximum tensile strength is 449.0, 114.3 and 306.2 MPa for Forearm Cuff, Forearm Linkage and Driven Joint respectively which are all smaller than 480.0 MPa of the yield strength of the ABS material. Therefore, ABS material is safety to use for the tennis application.

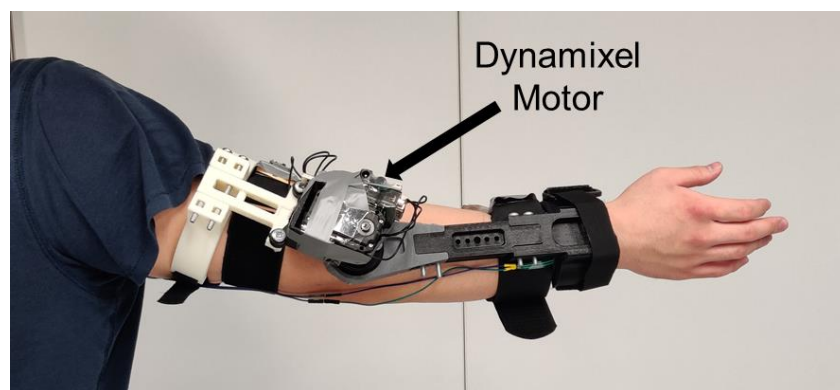


Fig. 10 Scene of Human Subject Wearing the Exoskeleton

According to the literature review, electric motor could be the most suitable choice for the actuator because it has relatively high accuracy control. However, the actuator for the upper limb sport application must have small weight and size in order to avoid interfacing the sport movement. In this project, the Dynamixel MX-64 motor has been chosen as the actuator which has the

100.71cm³ of volume. The motor could produce maximum continues torque of 3 Nm with the current of 0.3 A. Fig. 10 shown the picture of the scene of human subject wearing the exoskeleton and the position of the motor assembled to.

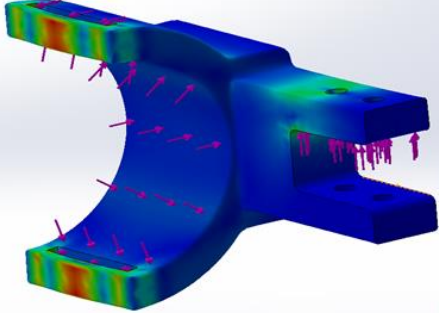
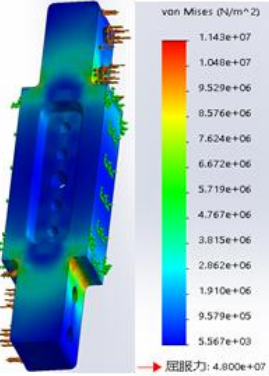
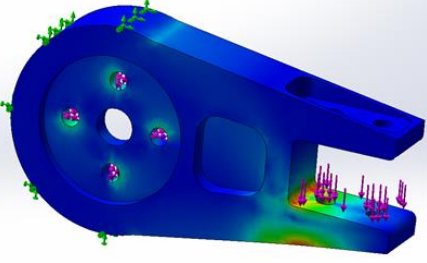
 <p style="text-align: center;">Forearm Cuff</p>	 <p style="text-align: center;">Forearm Linkage</p>	 <p style="text-align: center;">Driven Joint</p>
<p style="text-align: center;">Max. Tensile Strength =449.0 MPa</p>	<p style="text-align: center;">Max. Tensile Strength=114.3 MPa</p>	<p style="text-align: center;">Max. Tensile Strength =306.2 MPa</p>
<p style="text-align: center;">ABS Material Yield Strength=480.0 MPa</p>		

Table 3 FEA results compared with Yield strength of ABS material

Tennis Services Constrains:

The traditional damping torque is proportional and opposite to the motion of the mechanical plant shown in Eq1, where τ_d is the damping torque; w_{elbow} is elbow motion velocity; θ is the angular position; and $\theta_{threshold}$ is the threshold angular position where to apply the damping torque, In other words, the damping torque has linear relationship with the motion velocity. However, it goes against with the biology mechanical property of the relationship between muscle strength and muscle deformation speed. Most importantly, the damping torque applied cannot disturb the motion for the tennis serving and daily tasks. Therefore, it is hardly to define the coefficient for traditional damping torque.

$$\tau_d = \begin{cases} 0, & \theta \leq \theta_{threshold} \\ -k_d \times w_{elbow}, & \theta > \theta_{threshold} \end{cases}, \text{Eq1}$$

According to the literature reviews, there were already some researches about investigating the fuzzy logic applied to the exoskeleton controlling [43,44,45]. In the traditional control strategies, the control algorithm processes the discrete data to achieve the purpose of control. In other words, the traditional control strategies could work to the 'clear system'. However, the traditional control does not have strong capabilities when the system is 'fuzzy'.

The features of the fuzzy logic are that it adopts language rule based which is designed based on the user's knowledge and experience of the related application.[46] Also, it processes the fuzzy set class rather than exact discrete values. For an instance, in the water temperature and hot water pouring control application, the traditional control strategy deals with exact discrete temperature values in Celsius (i.e., 0 °C ~ 100 °C). In fuzzy logic, the controller processes with classes (i.e., named as 'Hot', 'Warm', etc.) as the degree of the water temperature then the class could be defuzzied into real discrete value for volume of hot water pouring output.

To design the fuzzy logic the first step is to define the input and output range. In this project, the input is the elbow motion velocity of elbow extension motion. For the output of the fuzzy logic, the output is the current of the motor. Because the motor torque output has positive correlation relationship with the current. According to the parameter of the Dynamixel MX-64 motor, it could provide the maximum continues torque with 300 of current of unt milliampere. Therefore, the minimum value of the current is 0 mA, and the maximum current output is 300 mA for maximum efficient torque applied to the damper.

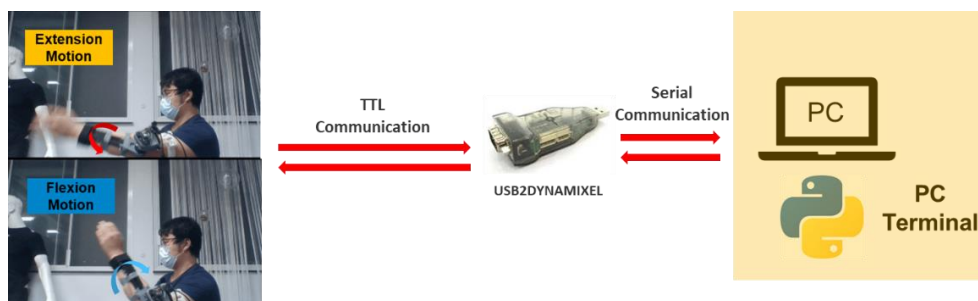


Fig. 61 Flow chart of elbow motion data acquiring

To design the fuzzy logic input range, an experiment for the elbow motion range (angular position range, and velocity range) is required. Fig. 11 shown the flow

chart of elbow data collection from the motor. The human subject did the extension and flexion motion with the assembled exoskeleton. The elbow angular position and motion velocity transmitted into PC terminal through USB2DYNAMIXEL with TTL communication. The data recorded with dynamixel python SDK with serial communication. The data plotting of the elbow motion shown in Fig. 12 which is made by MATLAB R2020a.

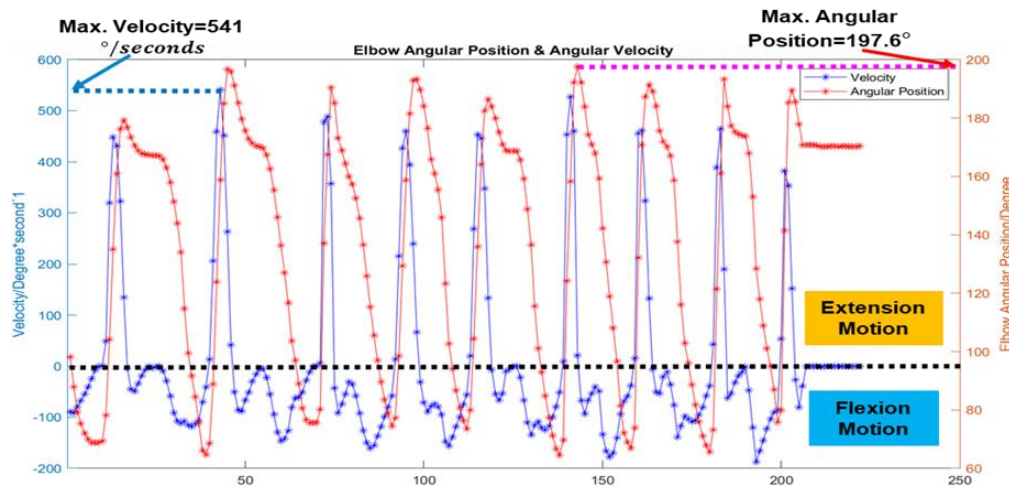


Fig. 17 Elbow motion plotting for fuzzy input range

It could be seen that the maximum elbow angular position reached to about 197.6 degree which is 17.6 degree above the normal fully extension elbow posture. Therefore, elbow overextension happened in this scenario. The black dot line draw at the zero velocity horizontally to classify the elbow extension and flexion motions. The origin of the velocity above the black dot line is the elbow extension scenario and the other region is elbow flexion scenario. Therefore, the minimum extension velocity is defined as zero and the maximum extension velocity is 541 degree per second.

The first step is necessary to decide an appropriate membership function. Normally, the common membership function for the fuzzy controllers is Triangular membership function, Trapezoidal membership function, Gaussian-shape membership function and Generalized Bell-shaped membership function [47]. S. Touil and D. Attous [48] investigated that the effect of different membership functions applied to fuzzy power system stabilizer of single machine infinite bus at Simulink environment. The results shown that the **triangular membership function has the shortest time of 3 seconds to damp the**

voltage output signal to stable state. For the trapezoidal membership function, it taken the longest about 9 seconds to make the voltage signal to be stable, which is three times slower than triangular membership function.

$$f(x, a, b, c) = \begin{cases} 0, & x \leq a \\ \frac{x-a}{b-a}, & a \leq x \leq b \\ \frac{c-x}{c-b}, & b \leq x \leq c \\ 0, & c \leq x \end{cases}, \text{Eq2}$$

Therefore, the triangular membership function is applied to this project for the elbow motion damper, the Eq2 shown the equation of the triangular membership function, where a, b and c determines the shape of the triangle, and (a, b, c) is set as crisp value range for one fuzzy set.

The next step of the fuzzy logic design is to define the fuzzy sets and rules. J. Zhao and B. Bose [49] proved that when number of the fuzzy set n=7 for both input and output, the indirect vector control for induction motor has the best performance while fuzzy set distribution is symmetric (Asymmetric factor =0). However, there is no research try to investigate the effect of different numbers of fuzzy sets to the damper performance.

	Input: Elbow Motion Velocity		Output: Current for Motor	
Rule	“ IF Input THEN Output ”			
	Crisp Input [a, b, c]	Fuzzy Set	Crisp Output [a, b, c]	Fuzzy Set
N=2	[0,180,360]	Slow	[0,100,200]	Small
	[180,360,540]	Fast	[100,200,300]	Large
N=3	[0,0,216]	Slow	[0,0,120]	Small
	[108,270,432]	Mid	[60,150,240]	Mid
	[324,540,540]	Fast	[180,300,300]	Large

N=5	[0,0,120]	Slow	[0,0,66.7]	Small
	[60,150,240]	Negative	[33.3,83.3,133.3]	R-Small
	[180,270,360]	Mid	[100,149.85,199.9]	Mid
	[300,390,480]	Positive	[166.5,216.5,266.5]	R-Large
	[420,540,540]	Fast	[233.2,300,300]	Large
N=7	[0,0,83]	Slow	[0,0,46]	Small
	[42,104,166]	Negative	[23,57.5,92]	R-Small
	[125,187,249]	Mid Neg	[69,103.5,138]	Mid Small
	[208,270,332]	Mid	[115,150,185]	Mid
	[291,353,415]	Mid Pos	[162,196.5,231]	Mid Large
	[374,436,498]	Positive	[208,242.5,277]	R-Large
	[457,540,540]	Fast	[254,300,300]	Large

Table 4 Parameters of Fuzzy Damper Experiment, where N=2,3,4 and 7

Therefore, another aim of this chapter is to investigate the effect of different number of fuzzy sets to the damper performance. According to [50], seven fuzzy sets has already produced a high accuracy induction motor control application. Therefore, it is not worthy to design the number of fuzzy set larger than seven.

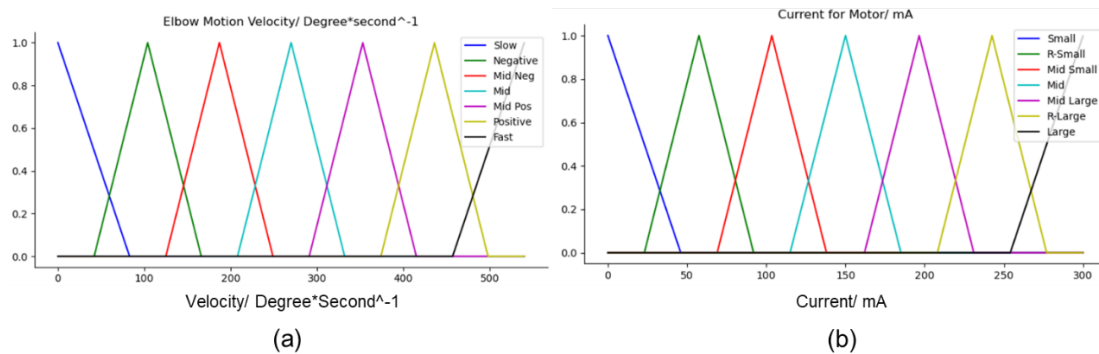


Fig 18 Triangular membership function plot for each fuzzy sets while N=7,(a) Input value, (b) Output value.

Table 4 shown the range of crisp input and output and names of different fuzzy sets for four experiments when the number of fuzzy sets (N) for input and output respectively. Fig. 13 (a) and Fig. 13(b) are draw with python shown the plots of triangular membership function for input and output while N=7, and the rest of the plots shown in the appendix (plotted by Python skfuzzy API) The x- axis is the crisp value of input and output values, and the y-axis is the degree of the

degree of membership function with range of (0 to 1). The rule for the fuzzy logic is set as “ IF Input THEN Output ” . Because the degree of the membership function for input should have positive correlation with output in order to produce same degree of elbow motion velocity and damping current (torque) of the motor. The last step for the fuzzy logic design is to define the defuzzification method. S. Naaz et al. [50] investigated that the effect to the output of different defuzzification methods applied on the fuzzy based balance control. It compared ‘Centroid’, ‘Bisector’, ‘MOM’, ‘LOM’, ‘SOM’. Among them, the ‘Centroid’, ‘Bisector’ and ‘MOM’ methods shown approximately same results of the output. But the ‘LOM’ and ‘SOM’ methods give larger variance in the results with same input.

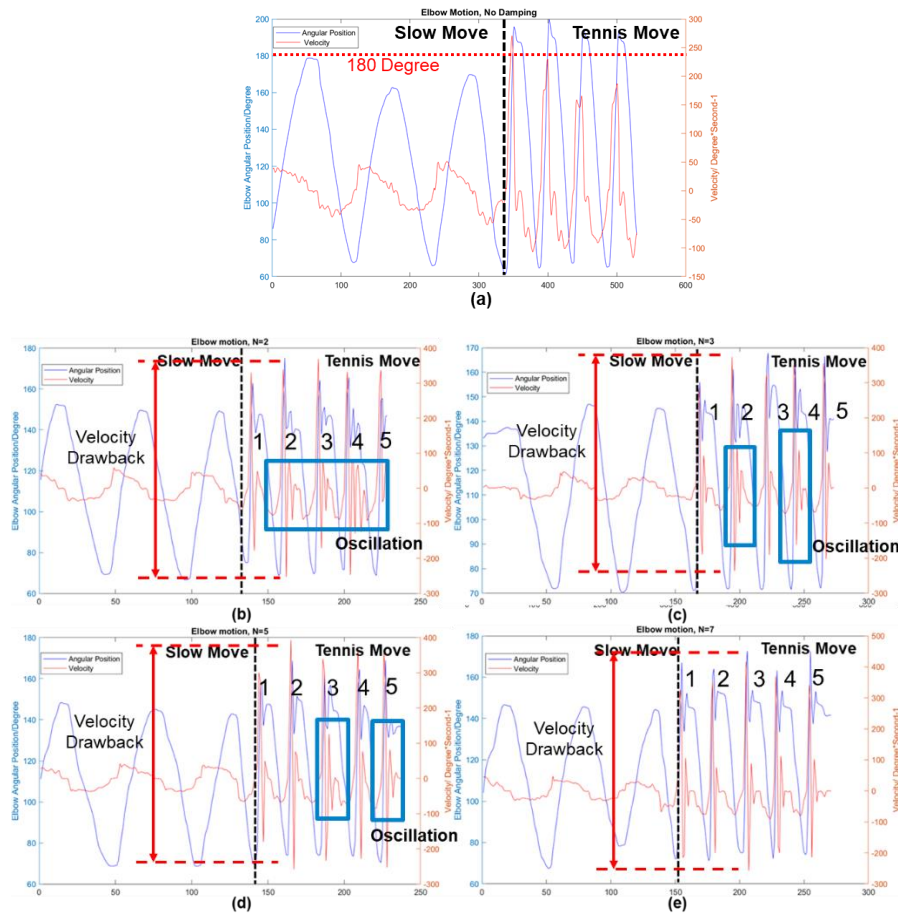


Fig. 19 (a). Elbow motion without damper; (b).Damping N=2; (c).Damping N=3; (d).Damping N=5; (e).Damping N=6

$$\tau_d = \begin{cases} 0 & , \text{elbow angular position} \leq 120^\circ \\ \text{Fuzzy Damper} & , \text{elbow angular position} > 120^\circ \end{cases} , \text{Eq3}$$

Therefore, 'Centroid', 'Bisector', 'MOM' are more reliable defuzzification methods. In this project, 'MOM' method is chosen for defuzzification and the concept of the 'MOM' defuzzification is to find the mean value of crisp output that has the maximum membership degree in the aggregation. Therefore, the Eq3. shown the criteria to stimulate the fuzzy logic damping. The damping will be stimulated when the elbow angular position greater than 120 degree. Just in case, the velocity could be accelerated higher enough to provide enough damping output from fuzzy logic before reach to 180 degree.

	Number of Tennis Move	Velocity Drawback (From Max to Min./ Degree*Second ⁻¹	Mean Velocity Drawback
N=2	1	508	519.0
	2	592	
	3	540	
	4	579	
	5	376	
N=3	1	475	533.8
	2	610	
	3	517	
	4	510	
	5	557	
N=5	1	481	582.6
	2	651	
	3	573	
	4	598	
	5	610	
N=7	1	541	578.2
	2	552	
	3	674	

	4	569	
	5	555	

Table 5 Velocity Drawback for each tennis movements and mean velocity drawback for each N

To validate the fuzzy logic damping, it is necessary to test with human object wearing the exoskeleton to simulate the tennis movement in real time and compare it when the damping logic is off. Human subjects did similar movement range and speed for each trails. Fig. 14a shown the fast and slow extension/flexion motion. Fig. 14 b, Fig. 14c, Fig. 14d and Fig.1 4e shown the elbow motion of three extension/ flexion slow movements and five tennis (fast) movements labelled with number (1,2,3,4,5) when N= 2, 3, 5 and 7 respectively at damping mode. It could be seen that in Fig. 14 a, there is elbow overextension at all tennis moves which is over 180 degree, and the extension motion (when velocity is positive) has a range of velocity from -220 to 363 degree/ second.

It is noticeable that the velocity drawback (determined as the velocity difference between maximum velocity and minimum velocity) of tennis movements happened at all damping models which prevents angular position of elbow beyond 180 degree. Therefore, the fuzzy logic damper successfully prevents elbow over extension.

Interestingly, there are oscillations of velocity at the tennis movements for some damping mode (N=2,3 and 5), which labelled with blue rectangles. This is because the exoskeleton is not enough tightly fixed to the limb. When the damping force is applied to the limb, there will be misalignment happened between fixed point of the exoskeleton and the limb, and it will continue until the time when the elbow joint is fully extended, and the damping force stops applying. However, the fixed point of the exoskeleton returns to its original position, and the returning speed has same direction with elbow joint extension. The position angle and the angle are still greater than the angle threshold at this moment. So, the damping force will be reapplied at this time, and the above steps are repeated until the speed damped into zero.

Due to the fact of misalignment between limb and exoskeleton, the best way to analyse the performance each fuzzy damper is to compare the velocity

drawback for each extension/ flexion motions at tennis move for each damper which shown in Table 5. The mean values of velocity drawback for all movements of fuzzy damping logic with $N=2, 3, 5, 7$ are 519.0, 533.8, 582.6 and 578.2 degree/ second respectively. There is increasing trend for the velocity drawback while the number of fuzzy set increasing. Therefore, the effect of increasing the number of fuzzy sets could lead larger deacceleration of elbow extension motion.

However, the limitation for the experiments is the velocity control for each tennis movement has not been controlled as exactly same for each trail, although to get mean velocity drawback of multiple trails for each N could reduce the effect of variance of velocity to the results. The potential solution to solve this problem could applied additional EMG sensor, which could directly measure the biological signal from muscle to describe the amount of damping force applied.

Post-Stroke Rehabilitation Mirror Therapy:

1. Introduction:

The concept of the mirror therapy by using the exoskeleton is that the exoskeleton forces the motion trajectory of affected limb to follow with the same motion trajectory as the healthy side of limb. Based on the motion symmetric property for both sides of the upper limb. The post-stroke patient doing the mirror therapy task could consciously try to control the motion of affected limb refer to the reaction force feedback from between the surfaces of limb and exoskeleton. Based on the neuroplasticity property, the patient could slowly recovery the control accuracy and be painless to for the affected limb. However, one of the biggest challenges is how the motion kinematics of healthy limb could be captured.

According to the [51], the IMU sensor has advantages of good self-independence which could work in most of the environment. This type of device has been widely used at application of inertial-only navigation, attitude estimation for drones and smartphone devices Therefore, the IMU sensor will be used for kinematics estimation in this project.

Normally, the IMU sensor has 6 degree of freedom of measurements (Accelerometer in X, Y, Z axis; Gyroscope in X, Y, Z about axis). However, there are some drift of integration for the gyroscope to get the angle and the reading from the accelerometer is easy to be disturbed by sudden and rapid movement. Therefore, the IMU sensor cannot get the accurate attitude directly. The conventional methods to avoid the problems above is to use algorithms to fuse the data reading from accelerometer and gyroscope based on software. Some MEMS IMU also integrated with Magnetometer and air pressure gauge which could allow to measure the heading attitude and height from sea level of the device coordinates [52].

Conventionally, there are several typical algorithms to measure the joint angle with two IMU devices such as Mahony Filter, Madgwick Filter, Kalman Filter or Extend Kalman Filter etc [53,54,55]. However, the main problems with those methods is the calibration is required before implementing those algorithms to the IMU sensors. The reason of requirement of calibration for IMU is there is bias of IMU devices reading while the device is at stable scenarios due to the quality of manufacturing. It could cause the error of data reading and attitude estimation. The calibration is the process to minimize the bias. Normally, the basic method of advanced MEMS IMU has pre-calibration at the factory by using mechanical calibration platform. However, the cost for the mechanical calibration platform leads high prize of the product (i.e. Xsens series IMU) [56]. It goes against the low-cost demand for this project. However, It is noticeable that the manually calibration for the cheap IMU device (i.e. Adafruit series IMU) calibration has related higher time cost. It also goes against criteria of the portable rehabilitation requirement. Therefore, the posture estimation technique needs to compromise the price and the time cost requirements. In this project, two IMUs (two 9 Dof Adafruit BNO055 IMU sensors) are chosen to express the kinematics of the upper limb.

Recently, machine learning approaches has been used for the human limb kinematics estimation with IMU sensor. The advantage of machine learning approach is that it could automatically analyse and optimize the model based on the training dataset feature for the specific application. Typically, the machine learning approaches are widely used for human activation recognition

classification application. The HMM could achieve above 95% accuracy for the hand gesture estimation and the SVM is able to determine the gait classification with around 99% accuracy [57,58]. However, the limitation for the traditional machine learning approaches is it could solve the problems of the classification for the prediction, but it is hardly to construct the model for the regression application. Although there are some supervised learning models could implement to the regression application such as traditional ANN type model (i.e., Multilayer Perceptron, CNN etc.). But the limitation for the traditional ANN type model is that it could lose the changes from the previous status to the current status for the continues data which is static.

In this project, the application is prediction of elbow motion (angular position) based on the IMU sensor. The IMU data output is continues with several features (Gyroscope, Accelerometer, etc.). The angular position of the elbow joint is based on the relative change of the IMU attitudes. In other word, the application requires a dynamic model which could analysis the temporal changes of IMU data output.

According to the literature review, RNN type (i.e., LSTM, GRU, Bid-LSTM etc.) model has been widely used for human limbs kinematics estimation. The advantage of RNN type network is that it could process a sequence of data instead of single data. In other word, the regression results include the history change of the data thus it is dynamic. Therefore, RNN type model could be the potential solution for this project.

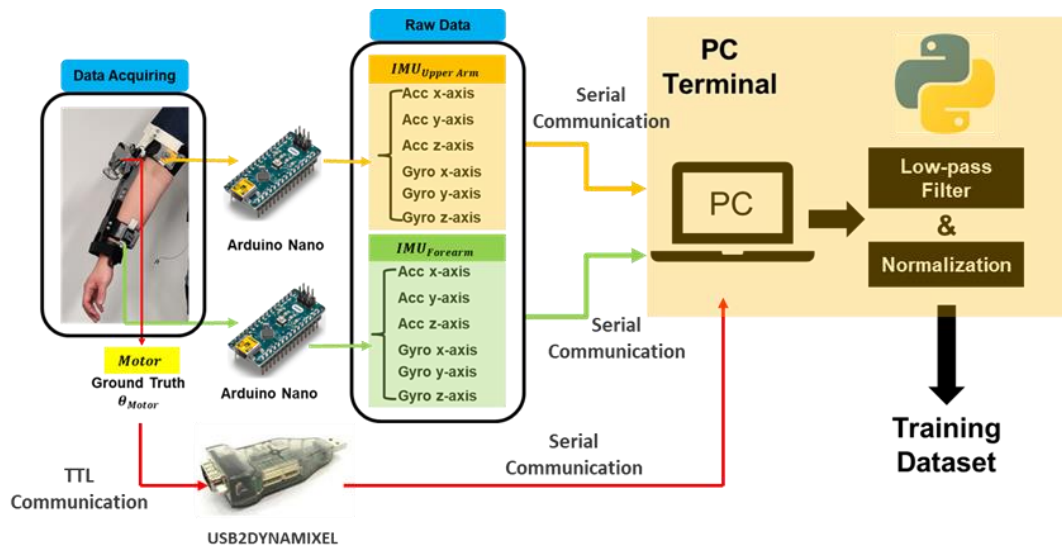


Fig. 105 Flow Chart of Data Acquiring and Pre-processing

2. Data Acquiring and Pre-processing:

To represent the kinematics of the elbow motion fully, it is necessary to place the two IMUs on the upper arm and forearm respectively in order to the two IMUs could move related to each other followed with the elbow joint. Fig.15 shown the flow chart of data acquiring and data pre-processing. The two IMUs connect with two Arduino Nano developer boards respectively, and the USB2DYNAMIXEL received the ground truth data of the elbow angle via TTL communication. Both raw data (all accelerometer readings and gyroscope readings from both IMUs) and ground truth angle from motor sent to the PC terminal through serial communication simultaneously.

All the data was sent to the python (3.7.9 Windows 10 64-bit) for data pre-processing with Min/Max Normalization so that speed up the convergence of the weight of the network. Additionally, a low pass filter has been applied to the data of the IMU to reduce the effect of the noisy input to the training disturbance since the accelerometer and gyroscope are easily get disturbance by sudden and rapid motion. The same human subject done the random elbow joint fully flexion & extension motion to accumulate the training data for 2 minutes with sampling rate 36 Hz. Fig.16 shown the plotting of elbow angle value received from motor.

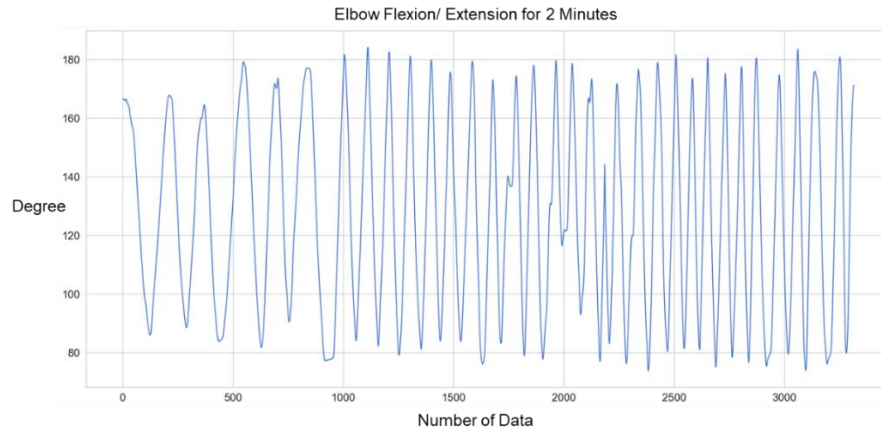


Fig. 16 Elbow Flexion/Extension of human subject for 2 minutes

3. Model construction:

In this project, Bid-LSTM has been chosen as the regression model to predict the elbow motion with IMU sensors. The traditional LSTM model only retains the past information according to the past input. The advantage of the Bid-LSTM model is that it not only covers the information from past but also the future status which has better higher accuracy at regression and classification application [59].

LSTM (Input), Act. =Relu	Units=512
Dense, Act. =Relu	Units=256
Dense, Act. =Relu	Units=128
Dense, Act. =Relu	Units=64
Dense, Act. =Relu	Units=32
Dense (Output), Act. =Linear	Units =2
Optimizer	Adam(lr=0.001)
Batch Size	500
Time Step	10
Loss Function	MSE

Table 6 Hyperparameter Initialization Network

4. Hyperparameters Tuning:

Artificial neuro network always be considered as black box operation. Fortunately, there are many research proved that tuning the parameters could optimize the accuracy of the model [60,61] (i.e. Act., lr, Batch Size, Time Step, Units). However, it will be token long time to construct and train an architecture from zero experiment. In order to reduce the training time, the initial model architecture can be used by other researchers to successfully deal with similar problems, and then the model can be optimized based on this original architecture. According to the research of R. Varghese et. al [62], they implemented a LSTM to predict the joint kinematics for the upper limb with the 2.51 and 1.33 of the RMSE of the 2 Dof shoulder kinematics which has related accurate prediction for the architecture. Therefore, the initialization could be referred to this architecture and the hyperparameters shown in Table 6 which has one LSTM layer with 512 units as the input layer and five dense layers afterwards with units 256,128, 64,32 and 2 respectively. All layers utilized Relu as the Act. except the output layer with Act. of Linear. It applied the Adam optimizer with learning rate of 0.001 and trained the model with batch size 500 and 10 timestep of LSTM. The loss function was MSE. In this project, the Bidirectional LSTM layer is applied to the input layer instead of LSTM and the output layer only has 1 unit since the model only output the elbow angle with one-dimension. The rest of the hyperparameters are same as the original architecture.

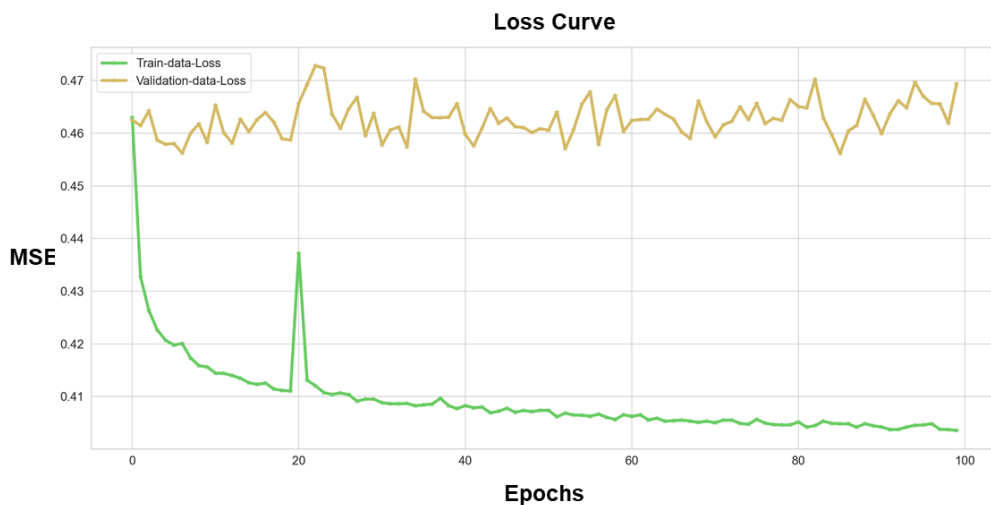


Fig. 17 Training loss curve for initial architecture network

The model has been constructed and trained with the Keras with the Tensorflow backend. Fig.17 shown the train-data and validation-data loss curves of original architecture. It could be seen that the loss curve for training data decrease during the epochs to converge at approximately 0.4036 of MSE. However, the validation loss curve does not have the trend of decrease, the MSE for first epoch is about 0.4624 and it is around 0.4694 of MSE at 100 epochs. The reduction of training data MSE approaches to -1.5% at the end of epoch. Therefore, the validation loss curve is rising with the decaying of the training loss curve. Thus, the model training resultant an overfitting [63]. The main possible reasons caused the overfitting of the model could be the structure of model is too complex, inappropriate learning rate and activation function etc., since the data amount is fixed, and the normalization of the data has been done [63].

Bid-LSTM (Input), Act. =tanh	Units=50
Dense, Act. = Relu	Units=30
Dense (Output), Act. =Linear	Units =1
Optimizer	Adam(lr=0.005)
Batch Size	50
Time Step	5
Loss Function	MSE

Table 7 Hyperparameters for optimized architecture after tuning

Therefore, the hyperparameters needs to be tuned. Table 7. shown the optimized architecture of the model after the tuning trails. The Bid-LSTM layer set as the input layer with units of 50 and the timestep is 5. The two additional dense layer with units 30 and 1 respectively. The optimizer for the model compiling kept as Adam with learning rate of 0.005 and the loss function kept as MSE.

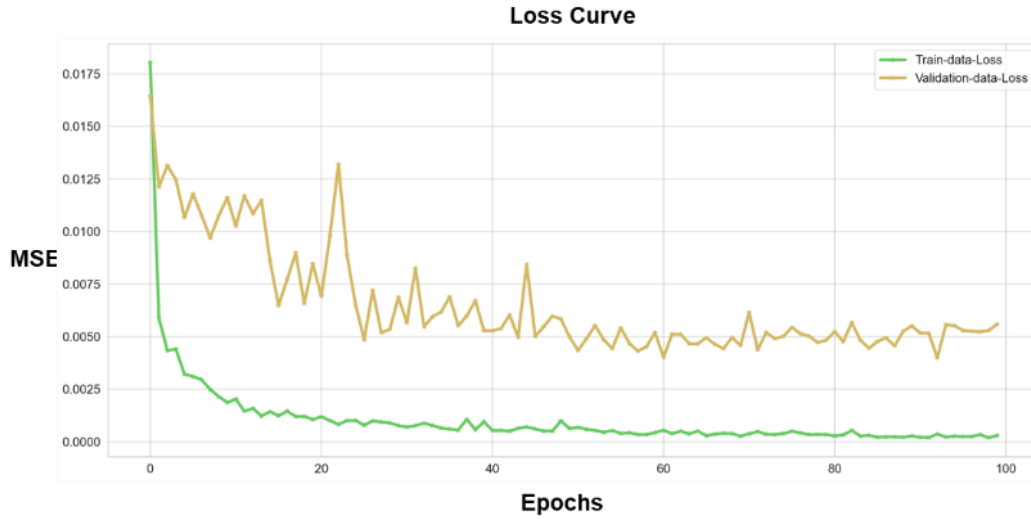


Fig. 18 Training loss curve for optimized architecture network after tuning

Fig. 18 shown the loss curve for train-data and validation-data with 100 epochs. It could be seen that the validation loss curve goes down with the train data loss decreased. At the beginning of the training, the MSE of the validation loss is 0.0165. It is noticeable that the train loss curve converged approximately to zero MSE at 100th epoch and the validation loss curve converged around 0.0050 MSE during the training, thus the validation MSE decreased by 69.7%. Therefore, the new architecture has been optimized successfully compared with overfitting property of original architecture and the schematic of the whole network structure shown in Fig. 19.

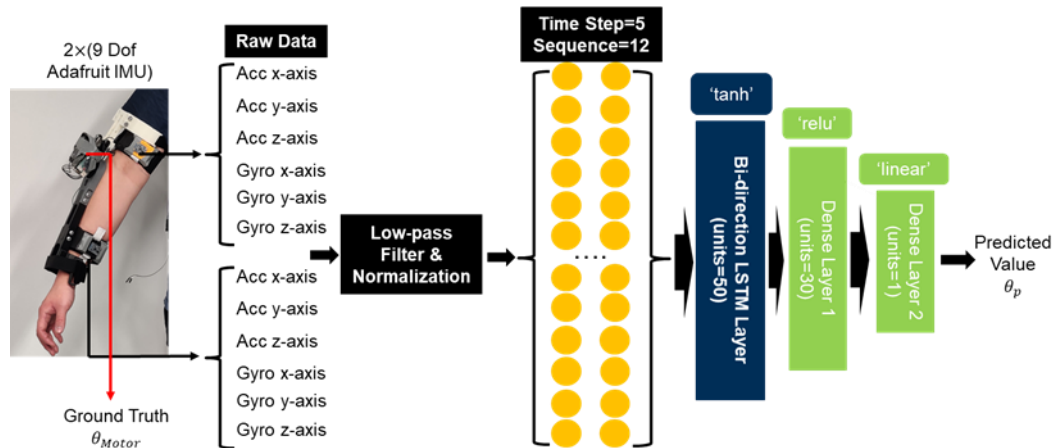


Fig. 19 Optimized Bidirectional LSTM Architecture

5. Real-time test:

To validate the accuracy of the model. A real-time test has been done with wearing the exoskeleton and IMU sensors with slow, fast and randomly fast flexion/extension elbow motion. Fig. 20 shown the curve of the predicted angle from the deep learning architecture and the real-time test true elbow angle read from the motor. The real-time test has been processed for 89.58 seconds. Among them, the slow elbow movement token 32.25 seconds, 22.70 seconds is the time spent of fast elbow movement and 34.63 seconds for randomly fast elbow movement. Fig. 21 shown the quartile box graph made by of the error between prediction angle and the test angle for the three types of elbow movements which is made by MATLAB R2020a. It could be seen that the slow elbow motion has smallest range of prediction error and the prediction error range getting larger at fast motion and randomly fast motion.

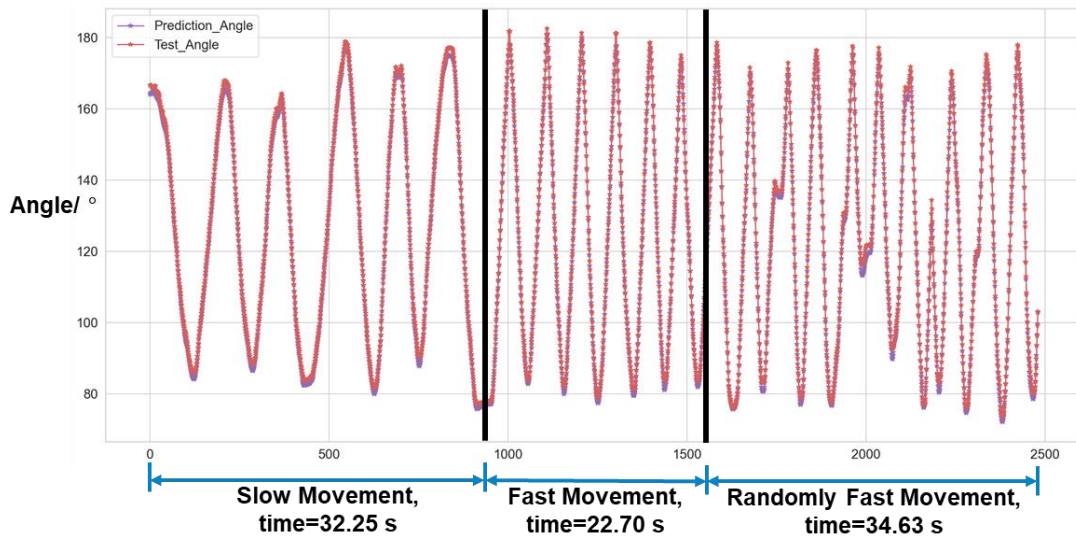


Fig. 20 Prediction and true angle of real-time test

The details of the quartile boxplot for the three motions shown in Table 8. The largest median of error for the slow motion with 1.38 degree and the randomly fast motion has the lowest median of the error at 1.07 degree. However, the highest IQR for randomly fast motion with 1.45 degree and the lowest IQR of 0.61 degree for slow elbow motion. It is also noticeable that the fast motion has the greater number of outliers than the other two type of motions which is 33. The RMSE is also calculated which is lowest at fast elbow motion and the RMSE for slow motion and randomly motion is 1.47 and 1.61 respectively.

Therefore, the deep learning model has the most stable prediction at slow elbow motion with smaller prediction error than the randomly fast motion. At the fast motion, the prediction of the model could reach to the lowest RMSE of 1.41 at fast motion but worse stability than the slow motion with 0.78 degree of IQR. For the randomly fast motion, the prediction RMSE could reach to 1.61 which is the highest at the three motions also it is most unstable for the prediction which has 1.45 degree of the IQR.

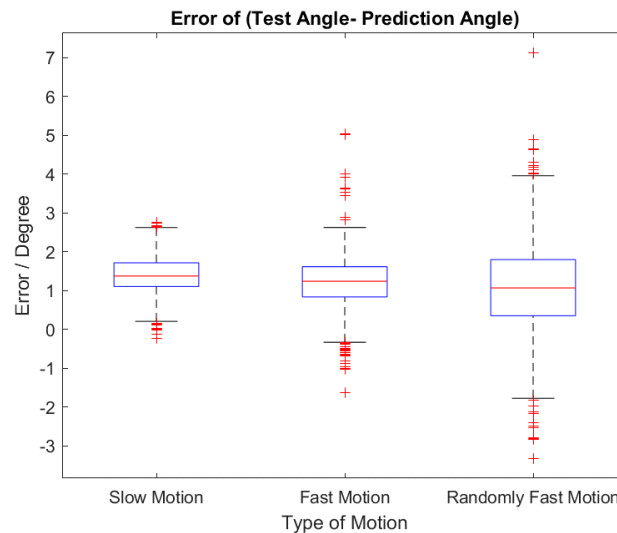


Fig. 21 Quartile box graph for three types of elbow motion

Therefore, the deep learning architecture could satisfy the elbow angle prediction at slow motion application, thus it could be applied to the post-stroke mirror therapy application. However, the architecture is relatively unreliable for the fast motion application such as the prediction of elbow angular position for tennis player.

	Slow Motion	Fast Motion	Randomly Fast Motion
Median(Q2)/ Degree	1.38	1.24	1.07
IQR(Q3-Q2)/ Degree	0.61	0.78	1.45
Number of Outliers	19	33	25
RMSE	1.47	1.41	1.61

Table 8 Details of the quartile plots and RMSE of the deep learning model at three types of motion

Conclusion:

The work presented in this paper demonstrates an exoskeleton for tennis and stroke patients' rehabilitation training. Its performance and control algorithm have undergone preliminary verification, proving its feasibility. Although more experiments are still needed to fully evaluate the performance of algorithms and hardware.

1. Summary of Achievement:

An 1-Dof exoskeleton for elbow joint has been designed and manufactured with ABS material, the elements could stand the load of tennis stroke torque.

For the application of tennis motion constrain, the damping algorithm accomplished with python Skfuzzy API. A real time test had been processed with a human subject to simulate the tennis movement while the damping mode switched on and off respectively. The fuzzy damping algorithm successfully prevent the over extension in tennis movement. The chapter 3 also investigated the effect of number of fuzzy sets to the damping output. It resultants increasing the number of fuzzy sets could lead larger deacceleration of elbow extension motion.

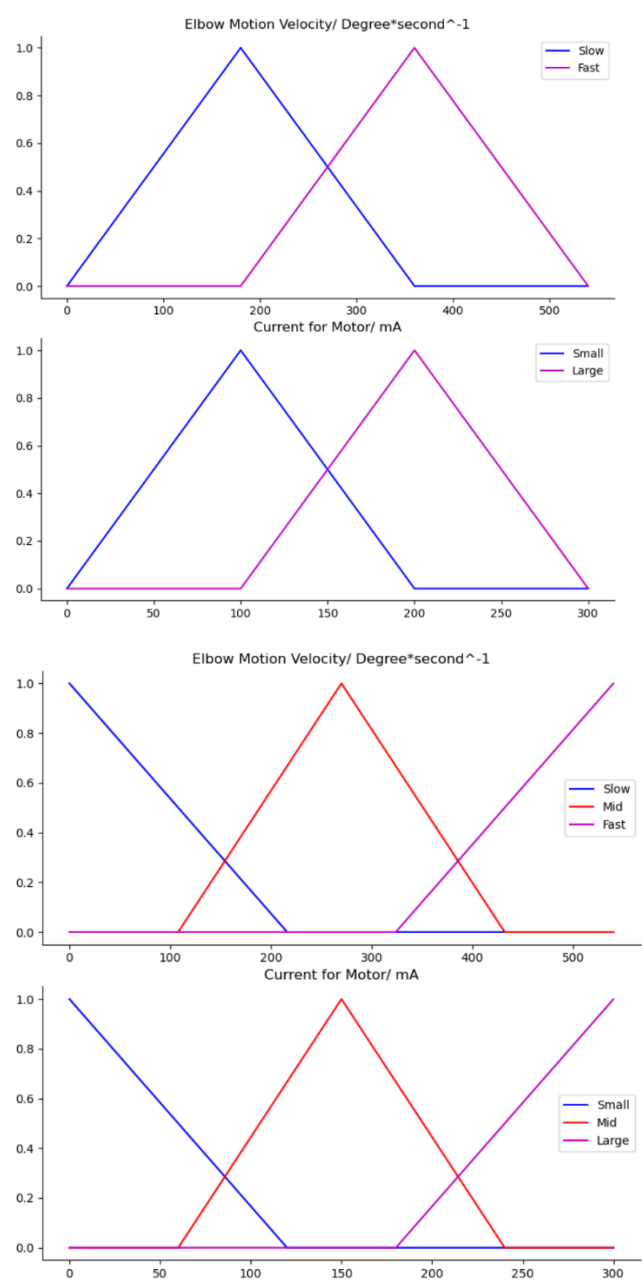
In the application of Post-Stroke Application. An architecture of Bid-LSTM accomplished by Keras API (Tensorflow Backend) for predicting the elbow angular position of the healthy limb. The model had been tested with a human subject to do three types of elbow movements (Slow Motion, Fast Motion and Randomly Fast Motion) in real-time. The results shown the model could have more accurate prediction at Fast Motion than other two. But the prediction is the stalest in Slow Motion.

2. Limitation and Future Work:

- The rigid exoskeleton cannot align with the shape of limb perfectly because there is always deformation of the limb due to the muscle contraction and relaxion. Also, it cannot perfectly tightly fixed with the limb. Therefore, it is worthy to try the soft wearable strategy such as the soft exo-sleeve.
- The validation of fuzzy damping needs a real-time test for real tennis playing scenario.

- To investigate the effect of fuzzy set to the fuzzy damping output. An additional EMG sensor could be applied on the limb to output a reaction of muscle directly. Also, it will be worthy to try the damping mode of soft exo-sleeve due to the oscillation effect by the rigid exoskeleton.
- The bidirectional LSTM model needs clinical test with post-stroke patients
- An extension of combination of bidirectional LSTM model and fuzzy damping is required. Because the ideal algorithm is the fuzzy damping could automatically switched on/off. Therefore, the potential solution could be changing the regression output layer of model into the classification (i.e. softmax) to classify the different phases of tennis serving.

Appendix:



•

[1]T. Ingall, "Stroke--incidence, mortality, morbidity and risk.", *Journal of insurance medicine*, vol. 362, pp. 143-52, 2004.

[2]T. Truelsen, B. Piechowski-Jozwiak, R. Bonita, C. Mathers, J. Bogousslavsky and G. Boysen, "Stroke incidence and prevalence in Europe: a review of available data", *European Journal of Neurology*, vol. 13, no. 6, pp. 581-598, 2006. Available: 10.1111/j.1468-1331.2006.01138.x.

[3]G Gresham, P Duncan, W Stason and A Adelman et al., "Post-Stroke Rehabilitation", *Rockville, MD, US Department of Health and Human Services, Public Health Service, Agency for Health Care Policy and Research*, 1995.

[4]H. Nakayama, H. Stig Jørgensen, H. Otto Raaschou and T. Skyhøj Olsen, "Recovery of upper extremity function in stroke patients: The Copenhagen stroke study", *Archives of Physical Medicine and Rehabilitation*, vol. 75, no. 4, pp. 394-398, 1994. Available: 10.1016/0003-9993(94)90161-9.

[5]K. Arya, S. Pandian, R. Verma and R. Garg, "Movement therapy induced neural reorganization and motor recovery in stroke: A review", *Journal of Bodywork and Movement Therapies*, vol. 15, no. 4, pp. 528-537, 2011. Available: 10.1016/j.jbmt.2011.01.023.

[6]L. Brewer, F. Horgan, A. Hickey and D. Williams, "Stroke rehabilitation: recent advances and future therapies", *QJM*, vol. 106, no. 1, pp. 11-25, 2012. Available: 10.1093/qjmed/hcs174.

[7]N. Bayona, J. Bitensky, K. Salter and R. Teasell, "The Role of Task-Specific Training in Rehabilitation Therapies", *Topics in Stroke Rehabilitation*, vol. 12, no. 3, pp. 58-65, 2005. Available: 10.1310/bqm5-6ygb-mvj5-wvcr.

[8]M. Alaverdashvili and I. Whishaw, "A behavioral method for identifying recovery and compensation: Hand use in a preclinical stroke model using the single pellet reaching task", *Neuroscience & Biobehavioral Reviews*, vol. 37, no. 5, pp. 950-967, 2013. Available: 10.1016/j.neubiorev.2013.03.026.

- [9]D. Ezendam, R. Bongers and M. Jannink, "Systematic review of the effectiveness of mirror therapy in upper extremity function", *Disability & Rehabilitation*, pp. 1-15, 2009. Available: 10.1080/09638280902887768.
- [10]T. Quinn, "Does mirror therapy improve motor function after a stroke?", *Cochrane Clinical Answers*, 2014. Available: 10.1002/cca.408.
- [11]J. Dines et al., "Tennis Injuries", *Journal of the American Academy of Orthopaedic Surgeons*, vol. 23, no. 3, pp. 181-189, 2015. Available: 10.5435/jaaos-d-13-00148.
- [12] G. Di Giacomo, T. Ellenbecker and W. Kibler, *Tennis Medicine*. Cham: Springer, 2019, pp. 286-288
- [13]Google.com,2020.[Online].Available:https://www.google.com/search?q=upper+limb+muscle+and+skeleton&sxsrf=ALeKk011cVqHvW1XPYySeMorQQf4a3G5DA:1582826765774&source=lnms&tbm=isch&sa=X&ved=2ahUKEwj0pfWYqfLnAhUVURUIHZVgAH4Q_AUoAXoECA0QAw&biw=1536&bih=722. [Accessed: 28- Feb- 2020].
- [14]W. Grana, "The Knee: Form, Function, and Ligament Reconstruction", *JAMA: The Journal of the American Medical Association*, vol. 250, no. 15, p. 2068, 1983. Available: 10.1001/jama.1983.03340150100047.
- [15]D. Neumann, *Kinesiology of the Musculoskeletal System Foundations for Rehabilitation*, 2nd ed. Elsevier Health Sciences, 2009.
- [16]A. Oosterwijk, M. Nieuwenhuis, C. van der Schans and L. Mouton, "Shoulder and elbow range of motion for the performance of activities of daily living: A systematic review", *Physiotherapy Theory and Practice*, vol. 34, no. 7, pp. 505-528, 2018.
- [17]K. Lee, J. Park, J. Beom and H. Park, "Design and Evaluation of Passive Shoulder Joint Tracking Module for Upper-Limb Rehabilitation Robots", *Frontiers in Neurorobotics*, vol. 12, 2018. Available: 10.3389/fnbot.2018.00038.
- [18]S. Namdari et al., "Defining functional shoulder range of motion for activities of daily living", *Journal of Shoulder and Elbow Surgery*, vol. 21, no. 9, pp. 1177-1183, 2012. Available: 10.1016/j.jse.2011.07.032.
- [19]E. Sarmiento, "Anatomy of the hominoid wrist joint: Its evolutionary and functional implications", *International Journal of Primatology*, vol. 9, no. 4, pp. 281-345, 1988. Available: 10.1007/bf02737381.
- [20]J. Ryu, W. Cooney, L. Askew, K. An and E. Chao, "Functional ranges of motion of the wrist joint", *The Journal of Hand Surgery*, vol. 16, no. 3, pp. 409-419, 1991. Available: 10.1016/0363-5023(91)90006-w.
- [21]B. Morrey and E. Chao, "Passive motion of the elbow joint", *The Journal of Bone & Joint Surgery*, vol. 58, no. 4, pp. 501-508, 1976. Available: 10.2106/00004623-197658040-00013.
- [22]J. Schmidt, *Hand and Upper Extremity Rehabilitation: A Practical Guide*, 4th ed. Elsevier Health Sciences, 2016, pp. 297-307.

[27]H. Kawamoto, Y. Sankai, S. Kanbe and Y. Sankai, "Power assist method for HAL-3 using EMG-based feedback controller", International Conference on Systems, Man and Cybernetics. Conference Theme - System Security and Assurance, vol. 2, pp. 1648-1653, 2003. Available: 10.1109/ICSMC.2003.1244649 [Accessed 18 February 2020].

[28]A. Zoss, H. Kazerooni and A. Chu, "Biomechanical design of the Berkeley lower extremity exoskeleton (BLEEX)", IEEE/ASME Transactions on Mechatronics, vol. 11, no. 2, pp. 128-138, 2006. Available: 10.1109/tmech.2006.871087.

[29] C.D. Takahashi, L. Der-Yeghian, V. Le, R.R. Motiwala, S.C. Cramer, Robot-based hand motor therapy after stroke, Brain 131, pp. 425–437, 2008 .

[30]Z. Li, C. Su, G. Li and H. Su, "Fuzzy Approximation-Based Adaptive Backstepping Control of an Exoskeleton for Human Upper Limbs", IEEE Transactions on Fuzzy Systems, vol. 23, no. 3, pp. 555-566, 2015. Available: 10.1109/tfuzz.2014.2317511.

[31]A. Stewart, C. Pretty, M. Adams and X. Chen, "Review of Upper Limb Hybrid Exoskeletons", IFAC-PapersOnLine, vol. 50, no. 1, pp. 15169-15178, 2017. Available: 10.1016/j.ifacol.2017.08.2266.

[32]S. Lessard, P. Pansodtee, A. Robbins, J. Trombadore, S. Kurniawan and M. Teodorescu, "A Soft Exosuit for Flexible Upper-Extremity Rehabilitation", IEEE Transactions on Neural Systems and Rehabilitation Engineering, vol. 26, no. 8, pp. 1604-1617, 2018. Available: 10.1109/tnsre.2018.2854219.

[33]M. Xiloyannis et al., "Design and Validation of a Modular One-To-Many Actuator for a Soft Wearable Exosuit", Frontiers in Neurorobotics, vol. 13, 2019. Available: 10.3389/fnbot.2019.00039.

[34]C. Thalman, J. Hsu, L. Snyder and P. Polygerinos, "Design of a Soft Ankle-Foot Orthosis Exosuit for Foot Drop Assistance", International Conference on Robotics and Automation (ICRA) Montreal, QC, Canada, 2019, pp. 8436-8442, 2019. Available: 10.1109/ICRA.2019.8794005 [Accessed 22 February 2020].

[35]P. Polygerinos, Z. Wang, K. Galloway, R. Wood and C. Walsh, "Soft robotic glove for combined assistance and at-home rehabilitation", Robotics and Autonomous Systems, vol. 73, pp. 135-143, 2015. Available: 10.1016/j.robot.2014.08.014.

[36]Y. Yang, D. Huang and X. Dong, "Robust Repetitive Learning Control of Lower Limb Exoskeleton with Hybrid Electro-hydraulic System," 2018 IEEE 7th Data Driven Control and Learning Systems Conference (DDCLS), Enshi, 2018, pp. 718-723.

[33]S. Lessard, P. Pansodtee, A. Robbins, J. Trombadore, S. Kurniawan and M. Teodorescu, "A Soft Exosuit for Flexible Upper-Extremity Rehabilitation", *IEEE Transactions on Neural Systems and Rehabilitation Engineering*, vol. 26, no. 8, pp. 1604-1617, 2018. Available: 10.1109/tnsre.2018.2854219.

[34]S. Yu et al., "Design and Control of a High-Torque and Highly Backdrivable Hybrid Soft Exoskeleton for Knee Injury Prevention During Squatting", *IEEE Robotics and Automation Letters*, vol. 4, no. 4, pp. 4579-4586, 2019. Available: 10.1109/lra.2019.2931427.

[35]L. Lu, Q. Wu, X. Chen, Z. Shao, B. Chen and H. Wu, "Development of a sEMG-based torque estimation control strategy for a soft elbow exoskeleton", *Robotics and Autonomous Systems*, vol. 111, pp. 88-98, 2019. Available: 10.1016/j.robot.2018.10.017.

[37]M. Hong, G. Kim and Y. Yoon, "ACE-Ankle: A Novel Sensorized RCM (Remote-Center-of-Motion) Ankle Mechanism for Military Purpose Exoskeleton", *Robotica*, vol. 37, no. 12, pp. 2209-2228, 2019. Available: 10.1017/s0263574719000845.

[38]K. Witte, S. Collins and A. Fatschel, "Design of a lightweight, tethered, torque-controlled knee exoskeleton.", *IEEE International Conference on Rehabilitation Robotics*, pp. 1646-1653, 2017. Available: 10.1109/icorr.2017.8009484 [Accessed 4 March 2020].

[39]M. Hong, G. Kim and Y. Yoon, "ACE-Ankle: A Novel Sensorized RCM (Remote-Center-of-Motion) Ankle Mechanism for Military Purpose Exoskeleton", *Robotica*, vol. 37, no. 12, pp. 2209-2228, 2019. Available: 10.1017/s0263574719000845.

[40]E. Marieb, P. Brady and J. Mallatt, *Human anatomy*. .

[41] A. McDaid, K. Kora, S. Xie, J. Lutz and M. Battley, "Human-inspired robotic exoskeleton (HuREx) for lower limb rehabilitation," *2013 IEEE International Conference on Mechatronics and Automation*, Takamatsu, 2013, pp. 19-24, doi: 10.1109/ICMA.2013.6617887.

[42]J. BURTON, R. PYE and D. BROOKES, "Metal corrosion by chloride in sweat", *British Journal of Dermatology*, vol. 95, no. 4, pp. 417-422, 1976. Available: 10.1111/j.1365-2133.1976.tb00843.x.

[43]Q. Wu, X. Wang, F. Du and R. Xi, "Modeling and position control of a therapeutic exoskeleton targeting upper extremity rehabilitation", *Proceedings of the Institution of Mechanical Engineers, Part C: Journal of Mechanical*

Engineering Science, vol. 231, no. 23, pp. 4360-4373, 2016. Available: 10.1177/0954406216668204.

[44]J. Narayan and S. Dwivedy, "Towards Neuro-Fuzzy Compensated PID Control of Lower Extremity Exoskeleton System for Passive Gait Rehabilitation", *IETE Journal of Research*, pp. 1-18, 2020. Available: 10.1080/03772063.2020.1838346.

[45]Q. Wu, X. Wang, B. Chen and H. Wu, "Development of an RBFN-based neural-fuzzy adaptive control strategy for an upper limb rehabilitation exoskeleton", *Mechatronics*, vol. 53, pp. 85-94, 2018. Available: 10.1016/j.mechatronics.2018.05.014.

[46]D. Rouvray, *Fuzzy logic in chemistry*. San Diego: Academic Press, 1997.

[47]W. Ling, *Nonlinear digital filters*. Amsterdam: Academic, 2007, pp. 8-31.

[48]S. Touil and D. Attous, "Effect of different membership functions on fuzzy power system stabilizer for synchronous machine connected to infinite bus", *International Journal of System Assurance Engineering and Management*, vol. 8, no. 1, pp. 255-264, 2015. Available: 10.1007/s13198-015-0344-8.

[49]J. Zhao and B. Bose, "Membership function distribution effect on fuzzy logic controlled induction motor drive", *Annual Conference of the IEEE Industrial Electronics Society*, vol. 1, pp. 214-219, 2003. Available: 10.1109/IECON.2003.1279982. [Accessed 17 December 2020].

[50]S. Naaz, A. Alam and R. Biswas, "Effect of different defuzzification methods in a fuzzy based load balancing application", *International Journal of Computer Science Issues*, vol. 8, no. 5, pp. 261-267, 2011. [Accessed 17 December 2020].

[53]J. Bergstra and Y. Bengio, "Random Search for Hyper-parameter Optimization", *Journal of Machine Learning Research*, vol. 13, pp. 281–305, 2012. [Accessed 12 December 2020].

[54]R. Varghese, A. Nguyen, E. Burdet, G. Yang and B. Lo, "Nonlinearity Compensation in A Multi-DoF Shoulder Sensing Exosuit For Real-Time Teleoperation", *IEEE RoboSoft*, 2020. [Accessed 13 December 2020].

- [55]K. Duan, S. Keerthi and A. Poo, "Evaluation of simple performance measures for tuning SVM hyperparameters", *Neurocomputing*, vol. 51, pp. 41-59, 2003. Available: 10.1016/s0925-2312(02)00601-x.
- [56]Y. Kim and a. Chung, "An Approach to Hyperparameter Optimization for the Objective Function in Machine Learning", *Electronics*, vol. 8, no. 11, p. 1267, 2019. Available: 10.3390/electronics8111267.
- [57]"Predicting Sentiment Polarity of Microblogs using an LSTM – CNN Deep Learning Model", *International Journal of Engineering and Advanced Technology*, vol. 8, no. 6, pp. 4368-4373, 2019. Available: 10.35940/ijeat.f8933.088619.
- [58]S. GARCIA, *DATA PREPROCESSING IN DATA MINING*. [Place of publication not identified]: SPRINGER INTERNATIONAL PU, 2016.
- [59]Y. Wang, A. Chernyshoff and A. Shkel, "Study on Estimation Errors in ZUPT-Aided Pedestrian Inertial Navigation Due to IMU Noises", *IEEE Transactions on Aerospace and Electronic Systems*, vol. 56, no. 3, pp. 2280-2291, 2020. Available: 10.1109/taes.2019.2946506.
- [60]J. Wendel, O. Meister, C. Schlaile and G. Trommer, "An integrated GPS/MEMS-IMU navigation system for an autonomous helicopter", *Aerospace Science and Technology*, vol. 10, no. 6, pp. 527-533, 2006. Available: 10.1016/j.ast.2006.04.002.
- [61]S. Wilson et al., "Formulation of a new gradient descent MARG orientation algorithm: Case study on robot teleoperation", *Mechanical Systems and Signal Processing*, vol. 130, pp. 183-200, 2019. Available: 10.1016/j.ymssp.2019.04.064.
- [62]C. Hide, T. Moore and M. Smith, "Adaptive Kalman Filtering for Low-cost INS/GPS", *Journal of Navigation*, vol. 56, no. 1, pp. 143-152, 2003. Available: 10.1017/s0373463302002151.
- [63]M. Alatise and G. Hancke, "Pose Estimation of a Mobile Robot Based on Fusion of IMU Data and Vision Data Using an Extended Kalman Filter", *Sensors*, vol. 17, no. 10, p. 2164, 2017. Available: 10.3390/s17102164.

- [64] Averil. B and Reston. VA, "Progress in astronautics and aeronautics, Fundamentals of high accuracy inertial navigation", *American Institute of Aeronautics and Astronautics, Inc.*, 1997. [Accessed 15 December 2020].
- [65]M. Atia et al., "A Low-Cost Lane-Determination System Using GNSS/IMU Fusion and HMM-Based Multistage Map Matching", *IEEE Transactions on Intelligent Transportation Systems*, vol. 18, no. 11, pp. 3027-3037, 2017. Available: 10.1109/tits.2017.2672541.
- [66]J. En, S. Lee and J. Seo, "An analysis of Speech Acts for Korean Using Support Vector Machines", *The KIPS Transactions:PartB*, vol. 12, no. 3, pp. 365-368, 2005. Available: 10.3745/kipstb.2005.12b.3.365.
- [67]Graves A, Fernández S, Schmidhuber J. Bidirectional LSTM networks for improved phoneme classification and recognition[C]//International Conference on Artificial Neural Networks. Springer, Berlin, Heidelberg, 2005: 799-804.